Received: 20 March 2018 | Revised: 4 July 2018 | Accepted: 9 July 2018

DOI: 10.1002/kin.21210

ARTICLE

WILEY

Synthesis of poly(methyl methacrylate) via ARGET ATRP and study of the effect of solvents and temperatures on its polymerization kinetics

Anjana Dhar[1] | Bishnu P. Koiry[2] | Dhruba J. Haloi[1]

[1]Department of Chemistry, Bodoland University, Kokrajhar, India

[2]B.Voc. Rubber Technology, Tripura University, Suryamaninagar, India

Correspondence
Dhruba J. Haloi, Department of Chemistry, Bodoland University, Kokrajhar 783 370, India.
Email: dhruba2k3@gmail.com

Funding information
Science & Engineering Research Board (SERB), Grant/Award Number: ECR/2015/000075

Abstract

This investigation reports the synthesis of poly(methyl methacrylate) via activators regenerated by electron transfer atom transfer radical polymerization (ARGET ATRP) and studies the effect of solvents and temperature on its polymerization kinetics. ARGET ATRP of methyl methacrylate (MMA) was carried out in different solvents and at different temperatures using $CuBr_2$ as catalyst in combination with *N*,*N*,*N*′,*N*″,*N*″-pentamethyldiethylenetriamine as a ligand. Methyl 2-chloro propionate was used as ATRP initiator and ascorbic acid was used as a reducing agent in the ARGET ATRP of MMA. The conversion was measured gravimetrically. The semilogarithmic plot of monomer conversion versus time was found to be linear, indicating that the polymerization follows first-order kinetics. The linear polymerization kinetic plot also indicates the controlled nature of the polymerization. *N*,*N*-Dimethylformamide (DMF), tetrahydrofuran (THF), toluene, and methyl ethyl ketone were used as solvents to study the effect on the polymerization kinetics. The effect of temperature on the kinetics of the polymerization was also studied at various temperatures. It has been observed that polymerization followed first-order kinetics in every case. The rate of polymerization was found to be highest ($k_{app} = 6.94 \times 10^{-3}$ min^{-1}) at a fixed temperature when DMF was used as solvent. Activation energies for ARGET ATRP of MMA were also calculated using the Arrhenius equation.

KEYWORDS

atom transfer radical polymerization, kinetics, methyl methacrylate, solvent effect

1 | INTRODUCTION

Over past few years, controlled radical polymerization (CRP) has become one of the most versatile methods for the synthesis of well-defined polymer composition, architectures, and functionalities.[1–4] The development of CRP techniques in the past decade has attracted the synthetic polymer scientists to synthesize novel polymers with controlled and desired properties.[2,5,6] In past few years, it has been witnessed rapid development of few new CRP methods. All of these methods are based on establishing a rapid dynamic equilibration between a minute amount of growing free radicals and a large majority of the dormant species.[7]

There are three major CRP methods. They are (1) atom transfer radical polymerization (ATRP) or degenerative transfer, when dormant species are alkyl halides, (2) reversible addition-fragmentation chain transfer process, and (3) nitroxide mediated polymerization or stable free radical polymerization, where dormant chains are thioesters and alkoxyamines, respectively.[8–12] Among the different CRP, ATRP is the most commonly used polymerization technique. It is applied to polymerize a wide range of monomers at a wide range of polymerization temperature (−20 to 200°C).[13,14] Also, the reagents used in ATRP are commercially available.[1,15] ATRP has successfully been applied to synthesize a wide range of polymers with varied molecular

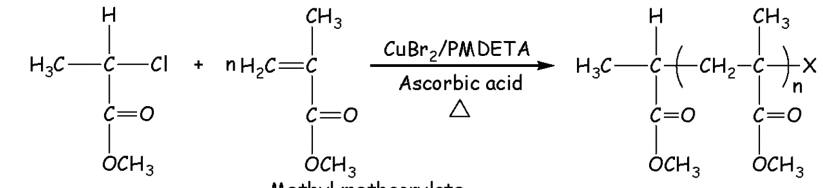

SCHEME 1 ARGET-ATRP of MMA

weights, different architectures, functionalities, and dispersity. Transition metal catalyzed CRP (commonly known as ATRP) is an important CRP method.[14,16] ATRP is carried out in the presence of an active alkyl halide using a transition metal halide as catalyst in combination with a suitable ligand.[14] There are several reports on the polymerization of different acrylate monomers using ATRP.[7,15–19]

ATRP is a repetitive transfer process of a halogen or pseudo-halogen atom between an alkyl halide R–X and a redox active transition metal complex Cu(I)X/ligand. The active species or radicals are generated by homolytic cleavage of alkyl halide R–X and are catalyzed by the transition metal complex (Cu(I)X/ligand). This process occurs with a rate constant for activation (k_a), propagation (k_p), deactivation (k_d), and the growing radicals terminate either by disproportionation or recombination (rate constant k_t).[1,2,7,20] In this process, the atom transfer step is the key elementary reaction step responsible for the uniform growth of the polymeric chains.[7] The presence of a metal catalyst limits the wider application of ATRP. However, attempts were made to recycle and reduce the use of catalysts.[20] These catalysts may add high cost to production, which may cause undesired cost to polymer.[5] Moreover, high conversions with control of polymer molecular weight become difficult with normal or conventional ATRP.[1]

So, different modified methods were developed with an aim either to reduce the concentration of catalyst or use of higher oxidation state air-stable catalyst. Few such methods are activators generated by electron transfer ATRP,[21b,c] activator regenerated by electron transfer (ARGET),[1c,13,21a,22] initiators for continuous activator regeneration ATRP,[1,23–27] supplemental activators and reducing agents ATRP,[23] etc.

In this work, use of ARGET ATRP is reported. Scheme 1 shows the ARGET ATRP of MMA along with the use of other ingredients. ARGET ATRP is one of the methods of ATRP that makes use of active catalyst in the ppm level. It also uses a reducing agent.[12] In this technique, the reducing agent regenerates the activator continuously maintaining the normal ATRP.[5] It is also possible to reduce the Cu catalyst even to very low ppm levels using the starting compound as an oxidatively stable deactivator species.[28] It has also been reported that ARGET ATRP can be used to synthesize polymer with high molecular weight.[13]

The monomer methyl methacrylate (MMA) is one of the highly used commercial monomer, which can undergo polymerization by all major techniques such as free radical, anionic, and group transfer polymerization.[30,31] The resultant homopolymer, poly(methyl methacrylate) has very high glass transition temperature (100–130°C) and possess the qualities that make it applicable in optics, pneumatic actuation, sensor, conductive devices, as additives in lubricants, etc.[29,30,32]

This study mainly focuses on the effect of solvents and polymerization temperatures on the ARGET ATRP of MMA.

2 | EXPERIMENTAL

2.1 | Materials

MMA (Aldrich; 99%, India) was purified by passing through basic alumina packed column and stored at 0°C. A ligand *N*,*N*″,*N*″,*N*′,*N*′-pentamethyldiethylenetriamine (PMDETA) (99%) was purchased from Sigma-Aldrich (India) and was used as received. Catalyst cupric bromide ($CuBr_2$) (99%; SRL, India) was used as received. Methyl-2-chloro propionate (MCP) (97%; Alfa Aesar, India) was used as received. *N*,*N*-Dimethylformamide (DMF) (99%; Emplura, India) was used as received. Other chemicals methanol (> 99%), L-ascorbic acid (99.7%) (Extrapure; AR) were purchased from SRL (India) and were used as received.

2.2 | ARGET ATRP of MMA

In a typical solution for polymerization, the catalyst $CuBr_2$ (0.1115 g, 0.50 mmol) and the ligand PMDETA (0.1298 g, 0.75 mmol) were taken in a dry Schlenk tube equipped with a magnetic stirring bar and the tube was then sealed with a rubber septum. Methanol (2 g) was injected to the Schlenk tube to dissolve the catalyst and ligand. This mixture was stirred for 10 min to form the catalyst/ligand complex. A solution of MMA (5 g, 0.05 mol) and initiator MCP (0.0612 g, 0.50 mmol) was then injected to the Schlenk tube. With continuous stirring, solvent toluene (5 g) and ascorbic acid (0.5 g, 2.83 mmol) were then injected to the Schlenk reaction tube

TABLE 1 Apparent rate constants of ARGET ATRP of MMA in different solvents and temperatures[a]

Experiment No.	Solvent	Temperature (°C)	Rate constant K_{app} (min^{-1})
1	*N*,*N*-Dimethylformamide	30	6.94×10^{-3}
2	Toluene	30	2.12×10^{-3}
3	Tetrahydrofuran	30	1.05×10^{-3}
4	Methylethyl ketone	30	1.04×10^{-3}
4a	Toluene	40	3.91×10^{-3}
4b	Toluene	50	5.71×10^{-3}
4c	Toluene	60	7.54×10^{-3}
4d	Toluene	70	1.23×10^{-2}

[a]Where [MMA]:[$CuBr_2$]:[PMDETA]:[MCP]:[Ascorbic Acid] = 100:1:1.5:1:5.

to start the polymerization. To carry out the polymerization at elevated temperature, the reaction tube was placed in an oil bath preheated at desired temperature. The aliquots were taken out at different polymerization times, and the conversion was determined gravimetrically.

3 | RESULTS AND DISCUSSION

3.1 | Polymerization kinetics

The polymerization kinetic results of ARGET ATRP of MMA are summarized in Table 1. The reactions were carried out in different solvents and at different temperatures. The relative molar concentrations of the ingredients were kept constant for all the experiments. Since, in ARGET ATRP, the rate of polymerization and the activator concentration increase with the presence of excess amount of ligand, therefore, the ligand was used at higher concentration as compared to the catalyst concentration in our case.

Ascorbic acid was chosen as reducing agent as it allows the reaction to restart by simply feeding into the reaction mixture if it is stopped at any point of time during the course of polymerization reaction.[33] The concentration of ascorbic acid was calculated on the basis of weight of all the ingredients to ensure a constant concentration regardless the size of the reaction batch.

3.2 | Nature of solvents

A series of solution polymerizations of MMA in a wide variety of polar and nonpolar solvents were carried out at ambient temperature to investigate the effect of the solvent on the ARGET ATRP process. In all cases, $CuBr_2$ was used as catalyst in combination with PMDETA as ligand at a molar ratio of [MMA]:[$CuBr_2$]:[PMDETA]:[MCP] is 100:1:1.5:1. DMF, toluene, tetrahydrofuran (THF), and methylethyl ketone were chosen as solvents for this study. The ambient temperature ARGET ATRP of MMA proceeds at faster rate in DMF as compared to other solvents used but toluene was chosen for studying the effect of temperature on polymerization. This is because, toluene has lower boiling point than DMF and it becomes easier to obtain the pure polymer when toluene is used as solvent.

Figure 1 shows linear semilogarithmic kinetic plots for all the four solvents. The linear dependency of $\ln(1-x)^{-1}$ (where x is the percentage of monomer conversion) with polymerization time indicates the first-order kinetics for the polymerization. The first-order kinetics is also the characteristics of a CRP. The apparent rate constant for the corresponding reactions were calculated from the slope of the plots and are shown in Table 1. The highest apparent rate constant was obtained for DMF (6.94×10^{-3} min^{-1}). It has been reported that on addition of a polar solvent accelerates the rate of polymerization of acrylates. The solubility of the catalyst in the reaction mixture is a very important factor to increase the polymerization rate and to reduce the polydispersity of the obtained polymer. Wang and Matyjaszewski studied the polymerization of MMA in various solvents with different polarities.[34] It was found that the system becomes more soluble as the polarity of the solvent increases.[34,35] Haloi and Singha reported that addition of a small amount of acetone helps in solubilizing the copper catalyst in 2-ethylhexyl acrylate (EHA) and increases the rate of ATRP of EHA.[36] The second best polymerization result in terms of the polymerization rate was achieved when toluene was used as solvent. It has also been reported that toluene complexes strongly with MMA,[37] and this has been reflected in the results shown in Table 1. Earlier, the change in the reaction rate was attributed to the effect of solvent in the initiation step.[38,39] But, Henrici-Olieve and Oleive proposed that it is the propagation step which is influenced by a solvent for formation of a complex between macroradical and either monomer or solvent molecule.[40] Bamford and Brumby have shown later that termination can be diffusion controlled, and it is the aromatic solvent that affects the k_p and k_t.[41] Burnet et al. showed that the effect of solvent is minor on initiation but has marked effect on propagation and termination.[42]

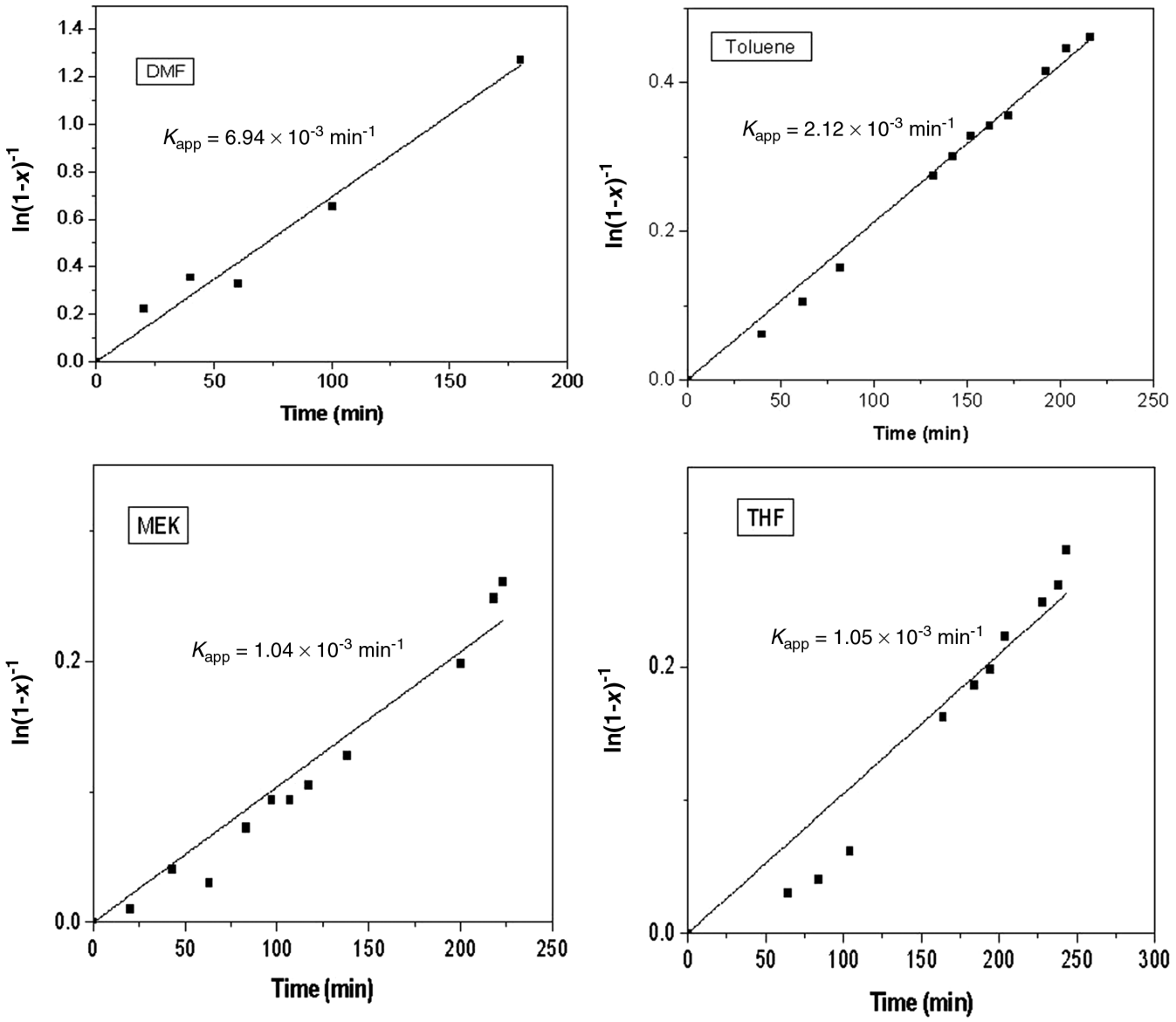

FIGURE 1 Kinetic plots for ARGET ATRP of MMA in different solvents at ambient temperature, where [MMA]:[CuBr2]:[PMDETA]:[MCP] is 100:1:1.5:1

Figure 2 shows the linear kinetic plots for all the five reactions carried out at different temperatures. In all cases, the plots are found to be linear, indicating the controlled nature of the polymerization. From the rearranged Arrhenius equation [$\ln k = -\frac{E_{act}}{R}\frac{1}{T} + \ln A$], a plot of $\ln A$ versus $1/T$ would give a straight line of slope equal to $-E_{act}/R$ (where terms have their usual significance). The slop obtained from this plot can be used to calculate the activation energy for the polymerization. Figure 3 shows the semilogarithmic plot of apparent rate constants versus the polymerization temperatures (in kelvins). The slope of this linear plot (–3984.0319) is used to calculate the activation energy. Thus the energy of activation for the ARGET ATRP of MMA in toluene is calculated to be 3.3123×10^4 J mol^{-1}.

4 | CONCLUSION

The ARGET ATRP of MMA was carried out successfully in different solvents and at different temperatures using $CuBr_2$/PMDETA as the catalyst system and MCP as the initiator. The effect of solvents on the polymerization rate was studied using four different solvents. At ambient temperature, DMF offers the fastest polymerization route among the four solvents as evident by the apparent rate constant value. It has also been established that successful polymerization in solution depends on the proper selection of solvent.

The kinetic plots were prepared by plotting conversion of monomer in percentage against the polymerization time. All the plots were found to be linear. This is the characteristics of

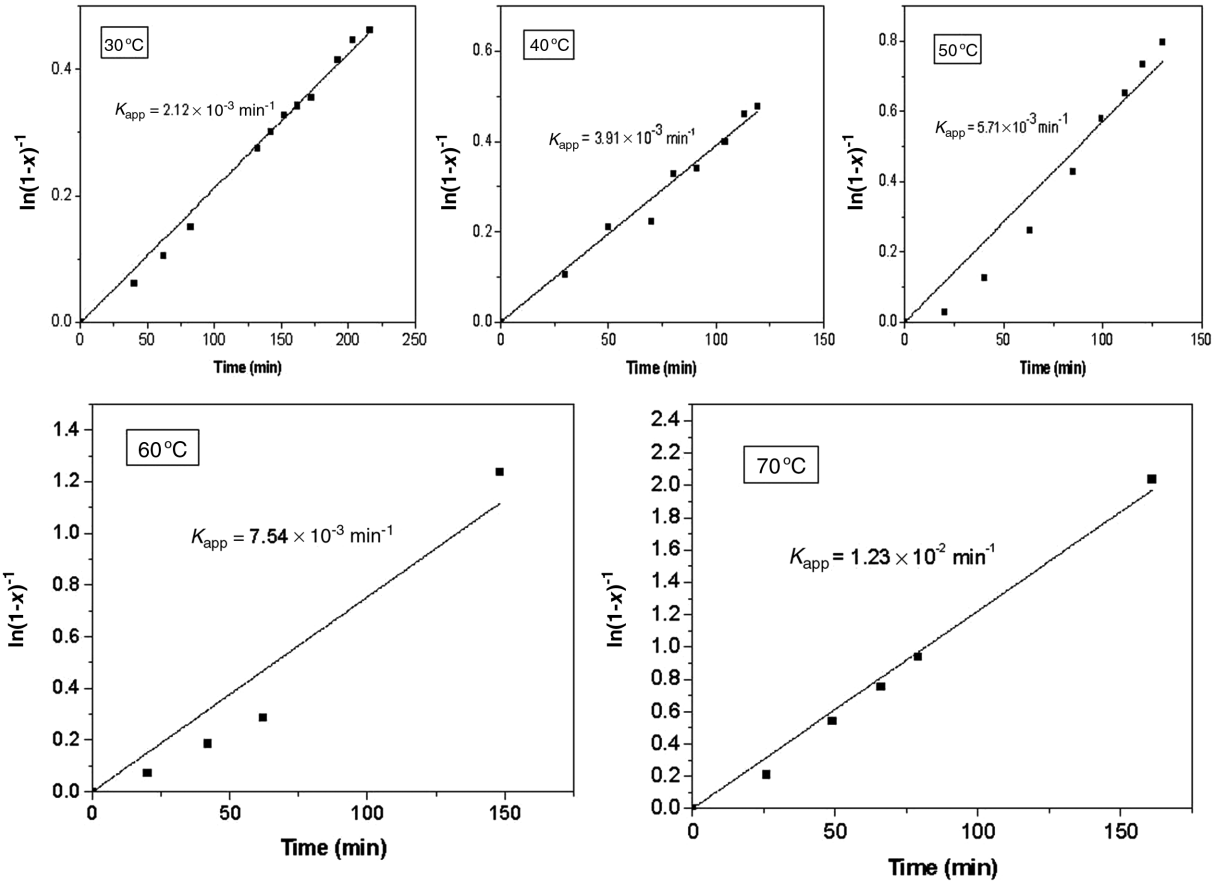

FIGURE 2 Kinetic plots of ARGET ATRP of MMA in toluene at different temperatures, where [MMA]:[CuBr2]:[PMDETA]:[MCP] is 100:1:1.5:1

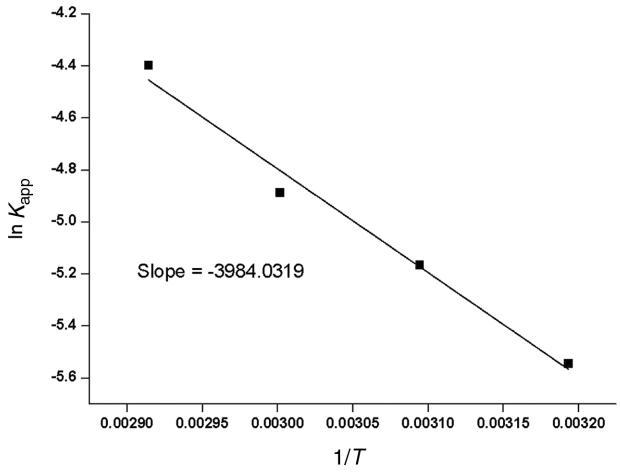

FIGURE 3 Semilogarithmic plot of apparent rate constants versus the polymerization temperatures (in Kelvins)

a first-order reaction and eventually establishes the controlled nature of the polymerization. The apparent rate constant for a particular polymerization was determined from the slop of the semilogarithmic kinetic plot and was used subsequently to calculate the activation energy.

ACKNOWLEDGMENT

The financial support from Science and Engineering Research Board (DST-SERB) (Grant no ECR/2015/000075), Government of India, is greatly appreciated.

ORCID

Dhruba J. Haloi http://orcid.org/0000-0002-4291-9328

REFERENCES

1. (a) Rabea AM, Zhu S. Controlled radical polymerization at high conversion: Bulk ICAR ATRP of methyl methacrylate. *Ind Eng Chem Res* 2014;53:3472−3477; (b) Haloi DJ, Ata S, Singha NK, et al. Acrylic AB and ABA block copolymers based on poly(2-ethylhexyl acrylate) (PEHA) and poly(methyl methacrylate) (PMMA) via ATRP. *ACS Appl Mater Interfaces* 2012;4:4200−4207; (c) Kwak Y, Matyjaszewski K. ARGET ATRP of methyl methacrylate in the presence of nitrogen-based ligands as reducing agent. *Polym Int* 2009;58:242–247.
2. Tsarevsky NV, Matyjaszewski K. Green atom transfer radical polymerization: From process design to preparation of well-defined environmentally friendly polymeric materials. *Chem Rev*. 2007;107:2270–2299.

3. D'Hooge DR, Steenberge PHMV, Reyniers MF, Marin GB. The strength of multi-scale modeling to unveil the complexity of radical polymerization. *Prog Polym Sci*. 2016;58:59–89.
4. D'Hooge DR, Steenberge PHMV, Derboven P, Reyniers MF, Marin GB. Model-based design of the polymer microstructure: Bridging the gap between polymer chemistry and engineering. *Polym Chem*. 2015;6:7081–7096.
5. Chan N, Cunningham MF, Hutchinson RA. ARGET ATRP of methacrylates and acrylates with stoichiometric ratios of ligand to copper. *Macromol Chem Phys*. 2008;209:1797–1805.
6. Matyjaszewski K, Tsarevsky NV, Braunecker WA, et al. Role of Cu0 in controlled/"living" radical polymerization. *Macromolecules*. 2007;40:7795–7806.
7. Matyjaszewski K, Jia J. Atom transfer radical polymerization. *Chem Rev*. 2001;101:2921−2990.
8. Steenberge PHMV, D'hooge DR, Wang Y, et al. Linear gradient quality of ATRP copolymer. *Macromolecules*. 2012;45:8519−8531.
9. Rahimi-Razin S, Haddadi-Asl V, Salami-Kalajahi M, Behboodi-Sadabad F, Roghani-Mamaqani H. Matrix-grafted multiwalled carbon nanotubes/poly(methyl methacrylate) nanocomposites synthesized by in situ RAFT polymerization: A kinetic study. *Int J Chem Kinet*. 2012;44:555–569.
10. Rybel ND, Steenberge PHMV, Reyniers MF, Kowollik CB, D'hooge DR, Marin GB. An update on the pivotal role of kinetic modeling for the mechanistic understanding and design of bulk and solution RAFT polymerization. *Macromol Theory Simul*. 2016;26:1600048.
11. Rybel ND, Steenberge PHMV, Reyniers MF, D'hooge DR, Marin GB. How chain length dependencies interfere with the bulk RAFT polymerization rate and microstructural control. *Chem Eng Sci*. 2018;177:163–179.
12. Steenberge PHMV, D'hooge DR, Reyniers MF, Marin GB, Cunningham MF. 4-dimensional modeling strategy for an improved understanding of miniemulsion NMP of acrylates initiated by SG1-macroinitiator. *Macromolecules*. 2014;47:7732–7741.
13. Bai L, Zhang L, Cheng Z, Zhu X. Activators generated by electron transfer for atom transfer radical polymerization: Recent advances in catalyst and polymer chemistry. *Polym Chem*. 2012;3:2685–2697.
14. Haloi DJ, Roy S, Singha NK. Copper catalyzed atom transfer radical copolymerization of glycidyl methacrylate and 2-ethylhexyl acrylate. *J Polym Sci Part A: Polym Chem*. 2009;47:6526–6533.
15. Braunecker WA, Matyjaszewski K. Controlled/living radical polymerization: Features, developments, and perspectives. *Prog Polym Sci*. 2007;32:93–146.
16. Matyjaszewski K (Ed.). *Controlled/Living Radical Polymerization: Progress in ATRP, NMP, and RAFT*. ACS Symposium Series, 768. Washington, DC: American Chemical Society; 2000. https://doi.org/10.1021/bk-2000-0768.
17. (a) Matyjaszewski K. Atom transfer radical polymerization (ATRP): Current status and future perspectives. *Macromolecules.* 2012;45:4015–4039; (b) Datta H, Singha NK. Atom transfer radical polymerization of hexyl acrylate; preparation of all-acrylate block copolymer. *J Polym Sci, Part A: Polym Chem.* 2008;46:3499–3511.
18. (a) Shipp DA, Wang J-L, Matyjaszewski K. Synthesis of acrylate and methacrylate block copolymers using atom transfer radical polymerization. *Macromolecules* 1998;31:8005–8008; (b) Singha NK, de Ruiter B, Schubert US. Atom transfer radical polymerization of 3-ethyl-3acryloyloxy methyloxetane. *Macromolecules.* 2005;38:3596–3600.
19. Zhang Y, Wang Y, Matyjaszewski K. ATRP of methyl acrylate with metallic zinc, magnesium, and iron as reducing agents and supplemental activators. *Macromolecules*. 2011;44:683–685.
20. Jakubowski W, Matyjaszewski K. Activators regenerated by electron transfer for atom-transfer radical polymerization of (meth)acrylates and related block copolymers. *Angew Chem*. 2006;118:4594–4598.
21. (a) Payne KA, D'hooge DR, Steenberge PHMV, et al. ARGET ATRP of butyl methacrylate: Utilizing kinetic modeling to understand experimental trends. *Macromolecules* 2013;46:3828–3840; (b) Hatami L, Haddadi-Asl V, Ahmadian-Alam L, Roghani-Mamaqani H, Salami-Kalajahi M. Effect of nanoclay on styrene and butyl acrylate AGET ATRP in miniemulsion: Study of nucleation type, kinetics, and polymerization control. *Int J Chem Kinet*. 2013;45:221–235; (c) Ahmadian-Alam L, Haddadi-Asl V, Hatami Hossein L, Roghani-Mamaqani H, Salami-Kalajahi M. Kinetic study of in situ normal and AGET atom transfer radical copolymerization of nbutyl acrylate and styrene: Effect of nanoclay loading and catalyst concentration. *Int J Chem Kinet.* 2012;44:789–799.
22. Payne KA, Steenberge PHMV, D'hooge DR, et al. Controlled synthesis of poly[(butyl methacrylate)-co-(butyl acrylate)] via activator regenerated by electron transfer atom transfer radical polymerization: Insights and improvement. *Polym Int*. 2014;63:848–857.
23. Boyer C, Corrigan AN, Jung K, et al. Copper-mediated living radical polymerization (atom transfer radical polymerization and copper(0) mediated polymerization): From fundamentals to bioapplications. *Chem Rev*. 2016;116:1803–1949.
24. Fierens SK, Steenberge PHMV, Reyniers MF, Marin GB, D'hooge DR. How penultimate monomer unit effects and initiator influence ICAR ATRP of n-butyl acrylate and methyl methacrylate. *AIChE J*. 2017;63:4721–5234.
25. D'hooge DR, Steenberge PHMV, Reyniers MF, Marin GB. Fed-batch control and visualization of monomer sequences of individual ICAR ATRP gradient copolymer chains. *Polymers*. 2014;6:1074–1095.
26. Porras CT, D'hooge DR, Steenberge PHMV, Reyniers MF, Marin GB. A theoretical exploration of the potential of ICAR ATRP for one- and two-pot synthesis of well-defined diblock copolymers. *Macromol React Eng*. 2013;7:311–326.
27. Porras CT, D'hooge DR, Steenberge PHMV, Reyniers MF, Marin GB. ICAR ATRP for estimation of intrinsic macroactivation/deactivation Arrhenius parameters under polymerization conditions. *Ind Eng Chem Res*. 2014;53:9674−9685.
28. (a) Jakubowski W, Min K, Matyjaszewski K. Activators regenerated by electron transfer for atom transfer radical polymerization of styrene. *Macromolecules*. 2006;39:39–45; (b) Jakubowski W, Matyjaszewski K. Activators generated by electron transfer for atom transfer radical polymerization. *Macromolecules*. 2005;38:4139–4146.
29. Hornby BD, West AG, Tom JC, Waterson C, Harrisson S, Perrier S. Copper(0)-mediated living radical polymerization of methyl

methacrylate in a non-polar solvent. *Macromol Rapid Commun*. 2010;31:1276–1280.

30. Ali U, Karim KJBA, Buang NA. A review of the properties and applications of poly (methyl methacrylate) (PMMA). *Polym Rev*. 2015;55:678–705.
31. Mccord EF, Anton WL, Wilczek L, et al. $^{'}$H and ^{13}CNMR of PMMA macro monomersand oligomers — end groups and tacticity. *Macromol Symp*. 1994;86:47–64.
32. Ghosh P, Das T, Nandi DJ. Synthesis characterization and viscosity studies of homopolymer of methyl methacrylate and copolymer of methyl methacrylate and styrene. *J Solution Chem*. 2011;40: 67–78.
33. Simakova A, Averick SE, Konkolewicz D, Matyjaszewski K. Aqueous arget ATRP. *Macromolecules*. 2012;45:6371–6379.
34. Wang Y, Matyjaszewski K. ATRP of MMA in polar solvents catalyzed by $FeBr_2$ without additional ligand. *Macromolecules*. 2010;43:4003–4005.
35. de la Fuente JL, Fernμndez-Sanz M, Fernμndez-García M, Madruga EL. Solvent effects on the synthesis of poly(methyl methacrylate) by atom-transfer radical polymerization (ATRP). *Macromol Chem Phys*. 2001;202:2565–2571.
36. Haloi DJ, Singha NK. Synthesis of poly(2-ethylhexyl acrylate)/clay nanocomposites by in situ living radical polymerization. *J Polym Sci, A: Polym Chem.* 2011;49:1564–1571.
37. Bawk CEH, Jakes WH, North AM. Low temperature polymerization of methyl methacrylate initiated by ethylsilver. *J Polym Sci*. 1962;58:335–350.
38. Anderson DB, Burnette GM, Gowan AC. Some novel effects in solution polymerization. *J Polym Sci*. 1963;1:1465–1470.
39. Burnette GM, Dailey WS, Pearson JM. Radical polymerization in halogenated solvents. Part 1.—Methyl methacrylate polymerization initiated by azoisobutyronitrile. *Trans Faraday Soc*. 1965;61:1216–1225.
40. (a) Henrici-Olive G, Olive SZ. About the influence of solvents in the radical polymerization III. Electron-donor-acceptor complexes between polymer radicals and solvent molecules and their effect on kinetic. *Phys Chem* 1965;47:286–298; (b) Henrici-Olive G, Olive SZ. About the solvent influence on the radical. IV. Electron donor acceptor complexes in styrene polymerization. *Phys Chem.* 1966;48:35–50; (c) Henrici-Olive G, Olive S. For the polymerization of methyl methacrylates in bromobenzene. *Makromolek Chem*. 1966;96:221–226.
41. Bamford CH, Brumby S. The effect of aromatic solvents on the absolute rate coefficients in the polymerization of methyl methacrylate at 25°C. *Makromolek Chem*. 1967;105:122–131.
42. Burnett GM, Cameron GG, Zafar MM. Polymerization of methyl methacrylate in solution. *Eur Polym J*. 1970;6:823–830.

How to cite this article: Dhar A, Koiry BP, Haloi DJ. Synthesis of poly(methyl methacrylate) via ARGET ATRP and study of the effect of solvents and temperatures on its polymerization kinetics. *Int J Chem Kinet*. 2018;1–7. https://doi.org/10.1002/kin.21210

Journal of Polymer Research (2020) 27:174
https://doi.org/10.1007/s10965-020-02153-x

ORIGINAL PAPER

Investigation of microstructure in poly(methyl methacrylate) prepared via ambient temperature ARGET-ATRP: a combined approach of 1D and 2D NMR spectroscopy

Anjana Dhar[1] · Upendra Singh[2] · Bishnu P. Koiry[3] · Bikash Baishya[2] · Dhruba J. Haloi[1]

Received: 22 December 2019 / Accepted: 6 May 2020

Abstract

This investigation reports the analysis of different microstructures present in poly(methyl methacrylate) (PMMA) using1D and 2D NMR spectroscopy. The PMMA used in this study has been prepared via activators regenerated by electron transfer atom transfer radical polymerization (ARGET-ATRP) in DMF at ambient temperature using methyl 2-chloro propionate (MCP) as initiator, $CuBr_2$ as catalyst in combination with N, N, N′, N′′, N′′- pentamethyldiethylenetriamine (PMDETA) as ligand and ascorbic acid as reducing agent.^{13}C NMR, which provides good information about tacticity of a polymer, has been used extensively along with ^{1}H NMR spectroscopy to extract the information about the different microstructures present in PMMA. Heteronuclear multiple-bond correlation (HMBC), heteronuclear single-quantum coherence (HSQC), and total correlation spectroscopy (TOCSY) were also used to study the position of protons, couplings with carbon etc. in the PMMA.

Keywords PMMA · ARGET-ATRP · ^{13}C NMR · HSQC · TOCSY · HMBC

Introduction

Polymers are widely prepared using conventional free radical polymerization which has limitations like uncontrolled molecular weight, molecular architecture and dispersity. But, with the advent of controlled radical polymerization (CRP) these limitations are mitigated. It helps in synthesizing polymers with controlled and desired properties. There are different types of CRPs methods has been established and among these, atom transfer radical polymerization (ATRP) is the most commonly used technique [1–3].

In ATRP a repetitive transfer process of a halogen or pseudo-halogen atom between an alkyl halide R-X and a redox active transition-metal complex Cu(I)X/ligand is takes place. But, it has a limitation of control of molecular weight at high conversion [4, 5].

To overcome this limitation and to prepare polymer with control over molecular weight a new technique viz. Activators Generated by Electron Transfer (ARGET) ATRP is used. Matyjaszewski et al. reported the synthesis of high molecular weight polymer using ARGET-ATRP technique [6]. In ARGET-ATRP there is use of higher oxidation state catalyst in ppm level and a proper reducing agent and free radical thermal initiator like AIBN [7, 8].

In this manuscript the microstructure of PMMA prepared via ARGET-ATRP has been studied. The term microstructure is used for the specific structure of the repeat unit and sequencing of the repeat unit. By definition, polymer is a large molecule consisting of small repeating units [9]. These units can arrange themselves in different ways along the backbone of the chain. This alignment of the repeating unit in the chain is described by polymer microstructure [10]. From the polymer microstructure various information like, tacticity, stereochemistry of different group, number-average sequence lengths and degree of polymerization can be obtained [10, 11]. It has strong influence on both physical and chemical properties of the polymer [12]. For example, the isotactic PMMA melts at 160 °C and syndiotactic PMMA at 200 °C; similarly, isotactic polystyrene melts at 240 °C and syndiotactic polystyrene at 200 °C. In addition, the crystallinity of the polymers also varies with the degree of the tacticity [13]. Hence, the study

✉ Dhruba J. Haloi
dhruba2k3@gmail.com

[1] Bodoland University, Assam 783370, India

[2] CBMR, Lucknow, Uttar Pradesh 226014, India

[3] Tripura University, Suryamaninagar, Tripura 799022, India

Published online: 30 June 2020

of microstructure is very important and it helps to understand the relationship between the polymer properties and its structure and to prepare a new copolymer of required physicochemical properties [11].

The study of microstructure of polymers for both homopolymer [9, 14] and copolymer [10, 15–17] is possible with NMR spectroscopy as the chemical shift obtained in NMR spectroscopy is affected by the configuration of the chain [14].

To elucidate the complete structure of the polymer using only ^{1}H NMR spectroscopy is not sufficient as major portion of the information remains unseen due to the presence of multiple peaks of broad range. Therefore ^{13} C NMR spectra are used along with ^{1}H NMR spectra to study the complete structure of polymer [13]. The ^{13}C NMR spectrum of polymer with carbonyl carbons e.g. acrylic polymer gives detailed information about uneven distribution of configurational sequences [14, 18, 19]. The microstructure of polymer obtained also varies with the type of polymerization techniques: syndiotactic polymer is mainly obtained from free radical polymerization technique, a range of tacticities can be obtained from anionic polymerization but PMMA formed via group transfer polymerization is mainly syndiotactic [20].

Experimental

Preparation of poly (methyl methacrylate)

PMMA ($\overline{M_n}$ =7700 *a. u.* , *PDI* = 1.55) used for this investigation was prepared via ambient temperature ARGET-ATRP as reported in our earlier report [21]. The structural characterization of the PMMA was carried out by ^{1}H and ^{13}C NMR spectroscopy.

Characterization

NMR spectroscopy

The 1D and 2D NMR spectra of PMMA were recorded on Bruker NMR Spectrometer in solvent $CDCl_3$. ^{1}H and ^{13}C experiments were carried out at frequencies of 400 and 800 MHz, respectively and calibrated with respect to the solvent signal. Gradient HMBC and HSQC experiments were recorded using the pulse sequence *hmbcgpndqf* and *hsqcetgp* of Bruker software, respectively. The spectra acquired in HMBC with 1200 increments in the F1 dimension and 1216 data points in F2 dimension. Total correlation spectroscopy (TOCSY) experiment was performed using standard pulse sequence of 8 scans, accumulated for 440 experiments with 1.5 delay time. HSQC experiment was acquired with 100 increment in F1 dimension and 1208 data points in F2 dimension.

Result and discussion

The tacticity of the polymer PMMA synthesized via ARGET-ATRP [21, 22] has been studied by ^{1}H and ^{13}C NMR spectroscopy. The ^{13}C NMR spectra of PMMA are divided into four resonance regions. The first region from 16 to 20 ppm is assigned to α-methyl carbon resonances, shown in Fig. 1a. The splitting in this region from low to high chemical shift is assigned to different tactic configurations: *rr, rm/mr* and *mm* triads. A single peak was observed for triad *rr* at 16.5 ppm and *mr* triad was observed to be splitted into two peaks at 18.8 and 19.0 ppm. Further, for *mm* triads, two obtained peaks at 21.2 and 21.7 ppm were assigned to *rmmr* and *rmmm/mmmr* pentads respectively as earlier assigned by A. S Brar [10].

The second region from 44 to 45.6 ppm is assigned to quaternary carbon shown in Fig. 1b. the peaks at 44.6, 44.9 and 45.6 ppm within this region are assigned to the *mm, rm/mr* and *rr* triads respectively. The third region for methylene and methoxy region is in the range of 52–55 ppm as shown in Fig. 1c. The single peak at 52.0 ppm was assigned to Methoxy (–OCH_3) group, while the peak in the large chemical shift region from 51.7–54.6 ppm is assigned to methylene carbon resonances. It has also been reported that tetrads will have the order *rmr, rrr, mmr, mrr, mmm* and *mrm* from high to low chemical shift [10]. As shown in Fig. 1d, the fourth region, from 176.5–179.0 ppm is assigned to carbonyl carbon. Three sets of resonances for Carbonyl carbon were observed from 176.3–176.6, 177.0–177.4 and 177.9–178.7 ppm and were assigned as *mm, rm/mr* and *rr* triads respectively. The peaks at 176.3, 176.4 and 176.6 ppm assigned to *rmmr, mmmr/rmmm* and *mmmm* pentads on splitting by the *mm* triads were observed. As the same peaks for *rrrr, rrrm/mrrr* and *mrrm* pentads of centered *rr* were observed at 178.0, 178.3 and 178.6 ppm respectively. The *mmrr/rmrr and mmrm + rmrm* pentads of centered *mr* triads with the different intensities were observed at 177.2 and 177.3 ppm.

Researchers have already discussed about the assignments of carbon of methylene group and reported about the order of the tetrads, that tetrads will have *rrr, rmr, mrr, mmr, mrm* and *mmm* order from high to low chemical shift [10]. HSQC provides correlation between carbon and its attached protons.

In PMMA, methylene proton depends on diad of repeating unit. There are two similar protons of methylene of *r* diad due to same environment of functional group. Therefore, there will be only one crosspeaks in 2D HSQC between methylene carbon and protons. But in case of *m* diad methylene protons will be different to each other due to different environment of functional groups. Therefore, in 2D HSQC two crosspeaks will be observed between methylene carbon and its corresponding attached protons.

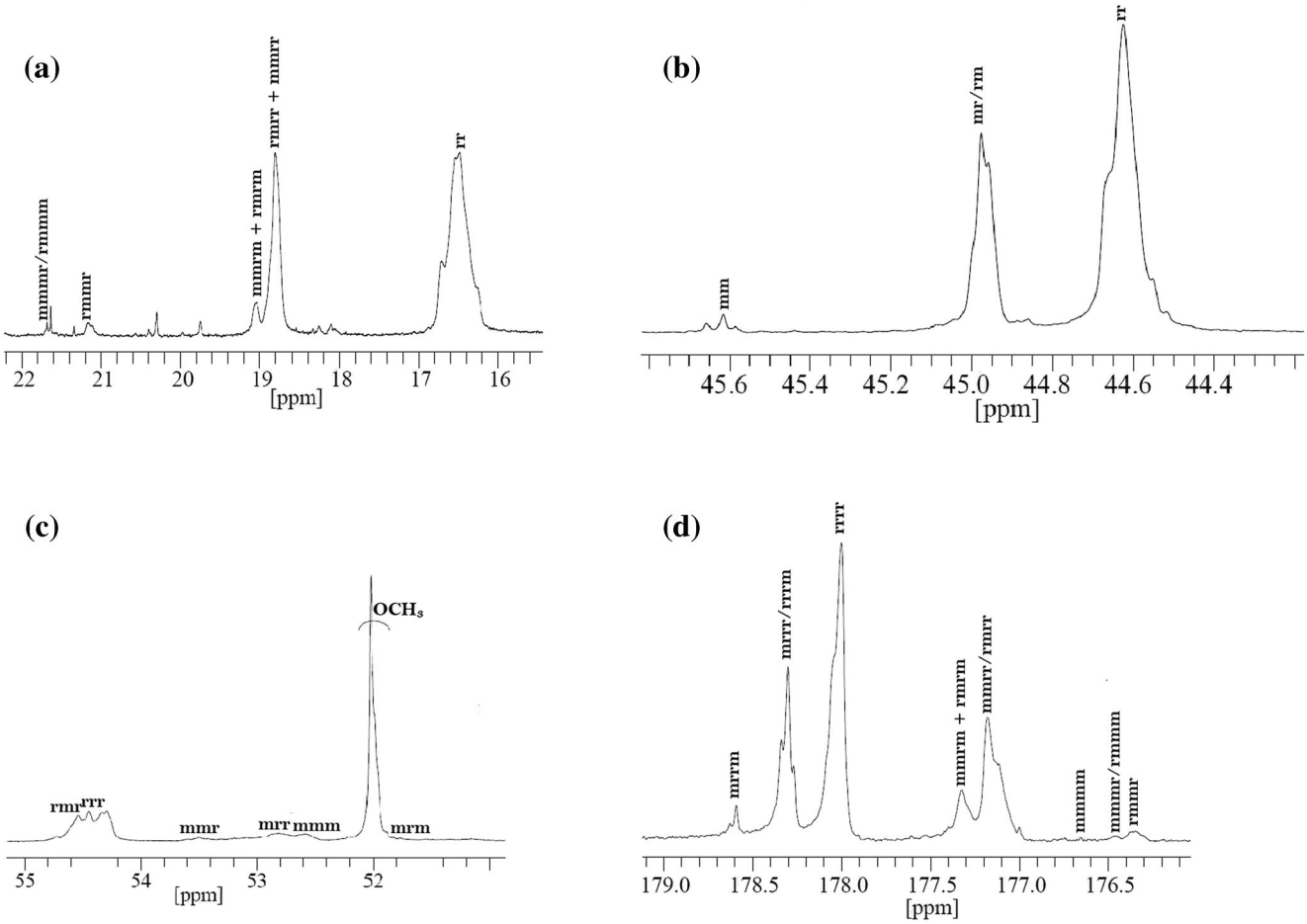

Fig. 1 Expanded ^{13}C NMR spectra of: (**a**) α-methyl carbon, (**b**) quaternary carbon. Expanded ^{13}C NMR spectra of (**c**) methylene and methoxy region, (**d**) carbonyl carbon region

2D HSQC study

The coupling of methylene region covering carbon resonances and proton resonances ranging from 51.0–54.5 ppm and 1.4–2.2 ppm is showed in the 2D HSQC spectrum Fig. 2. Direct attached carbon with protons (^{13}C-^{1}H) couplings between methylene carbon and proton are labeled from *A* to *I* in Schemes (1, 2 and 3) which resulted to corresponding crosspeaks shown in Fig. 2.

In Fig. 2, crosspeaks between methylene carbon and its protons *A* [as shown in Scheme 1a, b], proton *B* [as shown in Scheme 1b, c, 2a, b] and proton C [as shown in Scheme 2c, d] are seen.

Crosspeaks of couplings *D* and *E* [Scheme 2c] and *F* and *G* [Scheme 2a] observed for *rmr* tetrad and coupling *D/E* and *E/F* were assigned to H_A and H_B protons, respectively. The couplings *H* and *I* were assigned to H_A and H_B of *mmr* tetrad [Scheme 2b, d] and [Scheme 3a, b]. Crosspeaks *H* and *I* due to these couplings in 2D HSQC are shown in Fig. 2.

In 2D TOCSY spectrum two cross-correlation peaks are observed labeled as 'Y' between non-equivalent protons and the other labeled as 'X' is the result of another nonequivalent proton shown in Fig. 3.

The assignments of different interaction (Fig.4) using 2D TOCSY and HSQC NMR for 13C-labelled PMMA have been found consistent with some earlier reports [10].

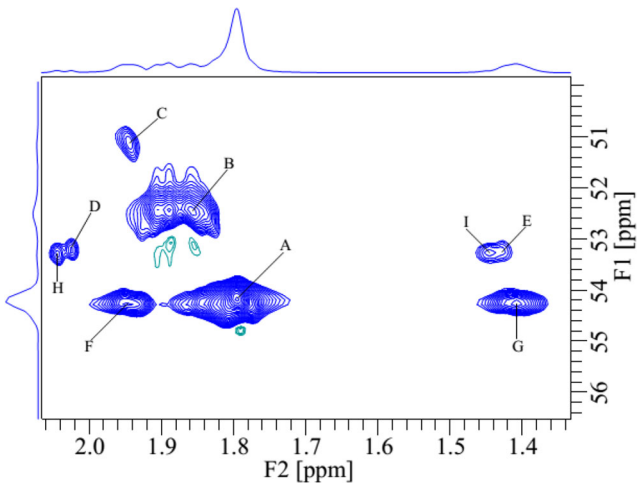

Fig. 2 The HSQC NMR spectrum of methylene region of PMMA

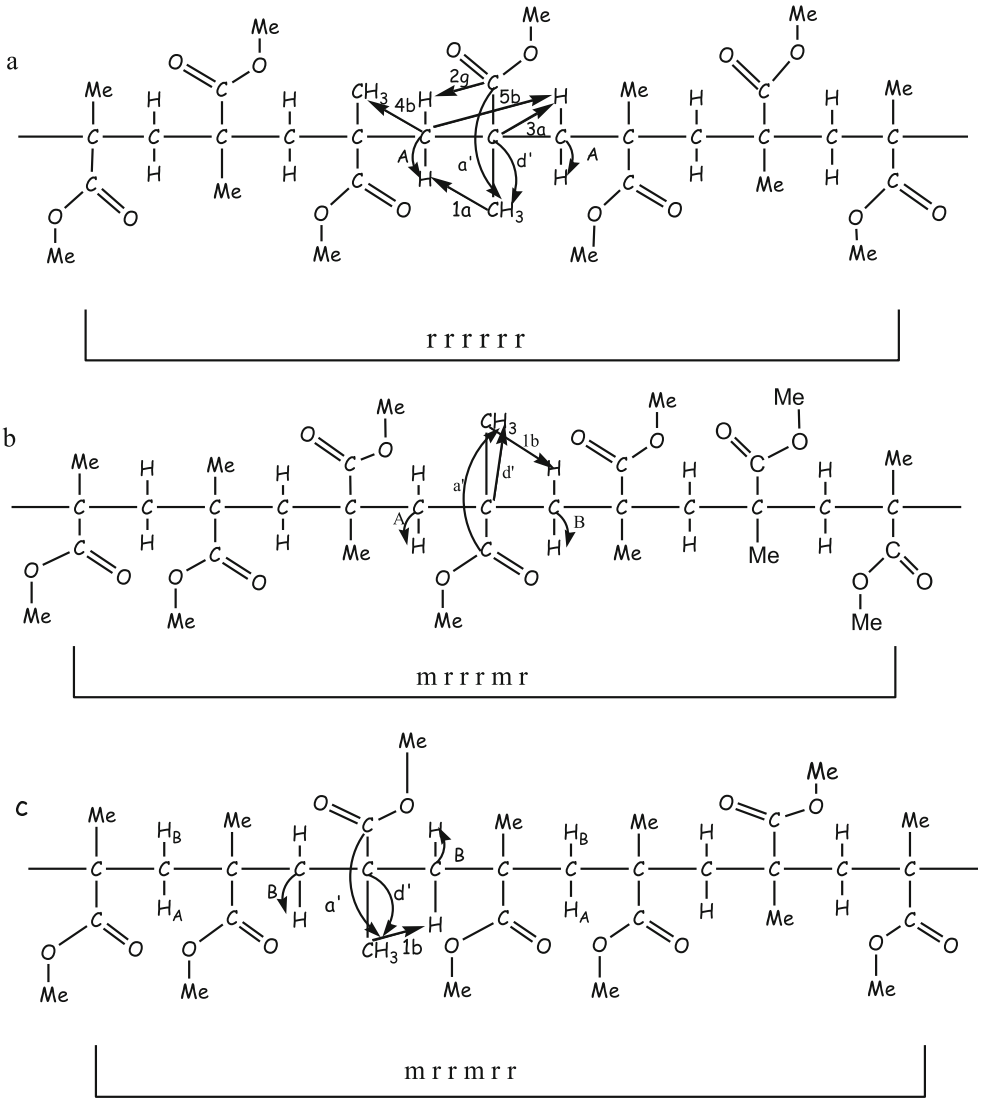

Scheme 1 Schematic representation of couplings in pentads with *rr* centered [10].

2D HMBC NMR experiment is a very useful method to study tacticity in high molecular weight polymer by extracting stereo chemical information [23]. This technique gives crosspeaks between carbon and proton that are separated by two, three and sometimes four bonds (in conjugated systems). The HMBC NMR spectrum of PMMA is shown in Fig. 5 and shows the couplings between carbon of α-methyl group and protons of methylene group of the molecule.Crosspeak *1a* is assigned to the coupling *1a* [Scheme 1a] between carbon of α-methyl group of *rr*-triad with protons of methylene group of *rrr* tetrad and crosspeak *1b* [Scheme 1b] and [Scheme 1c] for the coupling *1b* between *rr* of α-methyl carbon and *mrr* of methylene. The two resonance signals of triad *mr* is shown in Fig. 1b and further *mmrm* and *rrmr* pentads were assigned to signals at high and low chemical shift by comparing intensities of the signals [2]. The correlations between α-methyl carbon and methylene protons are very similar to those reported in the previous HMBC NMR result [10, 23].

In the 2D HMBC spectrum, the couplings *1e* and *1d* shown in Scheme 2a and couplings *1d* and *1f* shown in Scheme 2c corresponds to crosspeaks *1e* and *1d*, and crosspeaks *1e* and *1f* observed at low and high chemical shift signal. Further Brar et al. assigned the crosspeak 3, crosspeak 4, crosspeak 5 and crosspeak 6 to methylene of *rmr* tetrads by correlating HSQC and TOCSY spectrum. The crosspeaks *1 g* shown in Scheme 2a, b is for the coupling between *mr* carbon of α-methyl group with *mrr* proton of methylene group and the crosspeaks *1 h* Scheme 2c, d is assigned to *mrm* methylene.

Figure 6 shows the 2D HMBC spectrum of 3 bonds coupling of carbon of carbonyl group with protons of α-methyl group and with adjacent protons of methylene group. The coupling *a′* corresponding to crosspeak *a′* between protons of α-methyl group of *rr* triad with *rr* triad of carbonyl carbon is shown in Scheme 1 and the couplings *b′* and *c′* for *mr* and *mm* triads shown in Schemes 2 and 3 corresponds to crosspeaks *b′* and *c′*. The couplings *1j* and *2a* (Scheme 2a)

Scheme 2 Schematic representation of couplings in pentads with *mr* centered [10].

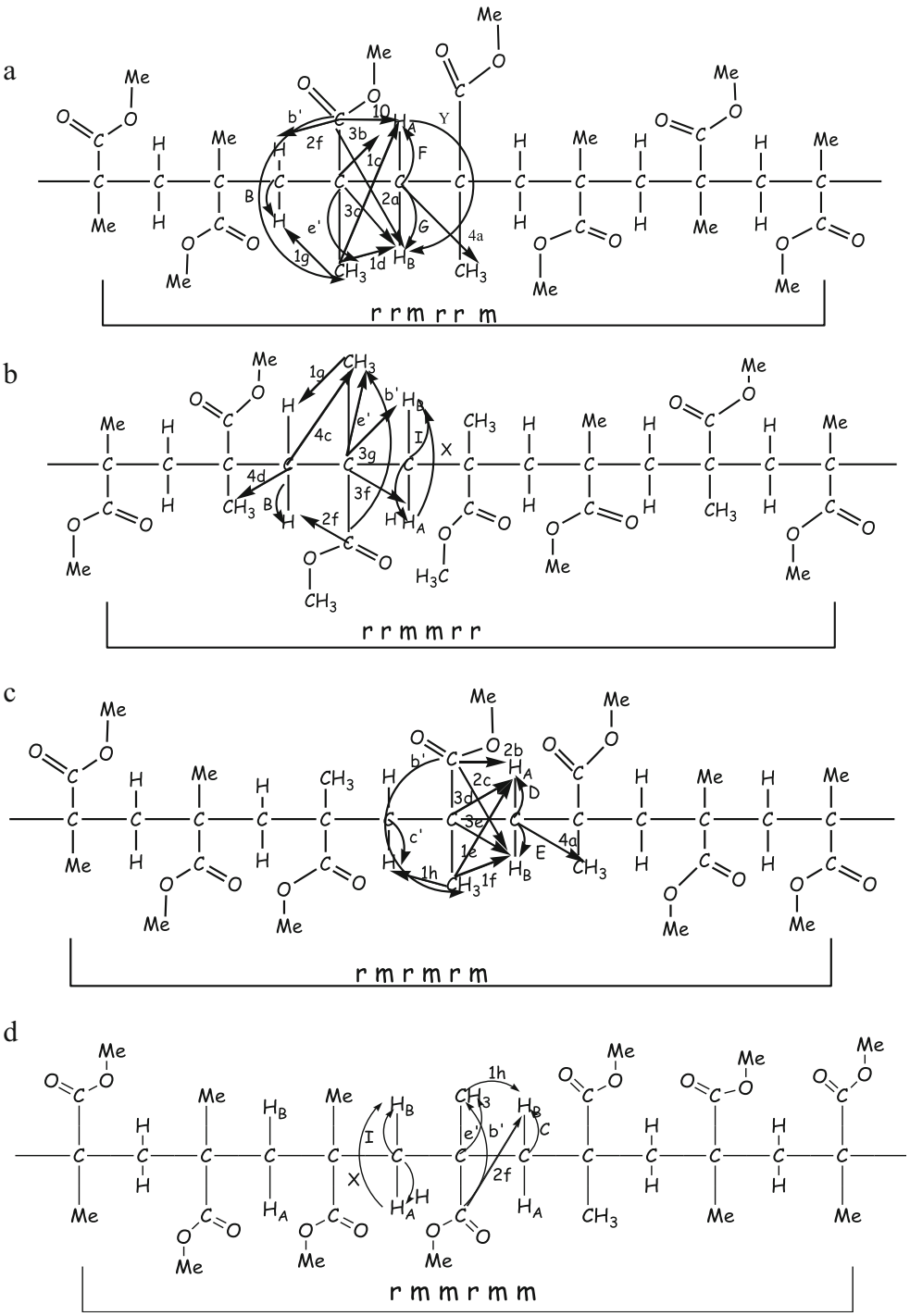

and couplings *2b* and *2c* (Scheme 2c) were assigned for *rmr* tetrad of *rmrr* and *rmrm* pentad based on the argument done by Brar et al. [10]. The couplings *1j*, *2a*, *2b* and *2c* correspond to crosspeaks *1j*, *2a*, *2b* and *2c* shown in Fig. 6. Coupling *2f* (Scheme 2a, b) between carbon of carbonyl group of *rrmr* or *mmrr* pentad and protons of methylene group of *mrr* tetrad corresponds to crosspeak *2 f*. Couplings *2d* and *2e* shown in Scheme 3a, b and coupling *2 g* (Scheme 1a) corresponds to crosspeaks *2d*, *2e* and *2 g*.

Figure 7 shows the 2D HMBC spectrum of PMMA. It shows couplings between carbon of quaternary and methylene group and protons of α- methyl group. Couplings *d′*, *e′* and *f′* (Schemes 1, 2 and 3) of the carbon of quaternary group with *rr, mr* and *mm* triads with protons of α- methyl group, respectively corresponds to crosspeaks *d′*, *e′* and *f′*.

Crosspeaks *3a, 3b, 3c, 3d, 3e, 3f* and *3 g* corresponds to couplings *3a, 3b, 3c, 3d, 3e, 3f* and *3 g* between quaternary carbon and methylene proton for different assignments of

Scheme 3 Schematic representation of couplings in pentads with *mm* centered [10].

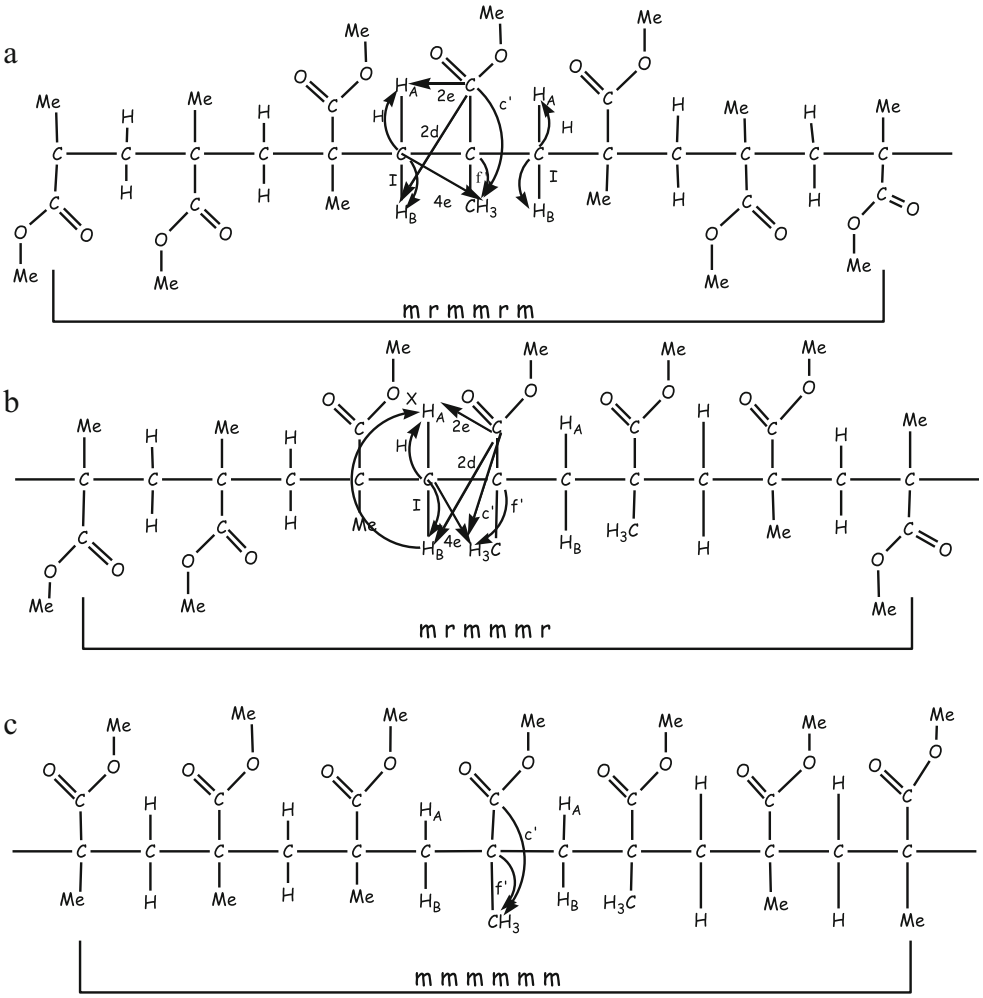

proton H_A and H_B of methylene. Coupling *3a* is shown in Schemes 1a, 3a, b in Scheme 2a, couplings *3d* and *3e* in Scheme 2c and couplings *3f* and *3 g* in Scheme 2b.

In Fig. 7 shows the couplings of α- methyl protons with methylene carbon. The crosspeaks *4a* (as shown in Scheme 2a, c), *4b* (as shown in Scheme 1a), *4c* and *4d* (shown in Scheme 2b) and *4e* (shown in Scheme 3a, b) corresponds to coupling *4a, 4b, 4c, 4d* and *4e*. The crosspeaks *4a* and *4b* are

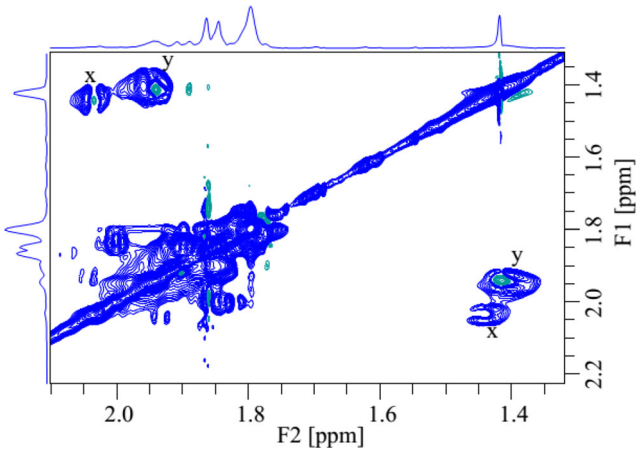

Fig. 3 2D TOCSY spectrum presentingcouplings of protons with *m* centered methylene tetrads in PMMA

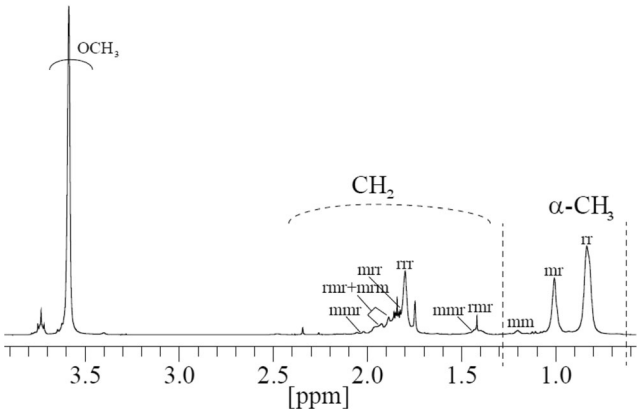

Fig. 4 ^{1}H NMR spectrum showing methylene and α-methyl protons of PMMA

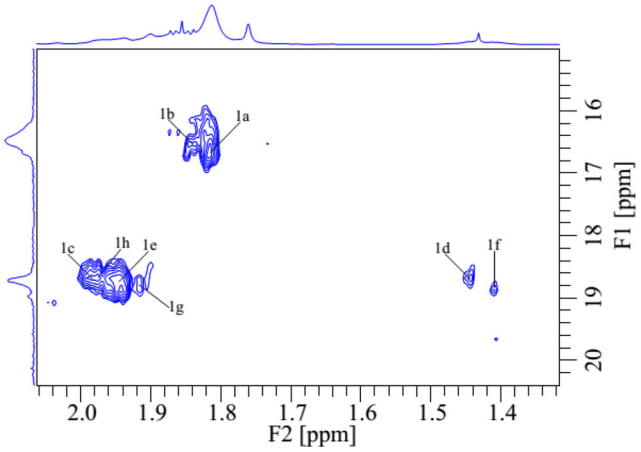

Fig. 5 2D HMBC spectrum presenting three bond couplings between α-methyl carbon and methylene protons

assigned to interaction of *rmr* and *mrr* of methylene carbon with α- methyl protons in *mr* configuration. While crosspeaks *4d* and *4e* are assigned to interaction of carbon of methylene group with *mrr* and *mmr* tetrad with protons of α- methyl group with *rr* and *mm* diad configuration, respectively. The crosspeak *5a* is due to the interaction of either *rrr* or *rmr* tetrad carbon with *mrm* tetrad proton, thus it is not assigned particularly and the crosspeak *5b* is assigned to interaction of *rrr* carbon with *rrr* methylene tetrad, respectively. The crosspeaks obtained and discussed were similar to that obtained by Brar et al. [10] and Kawamura et al. [24].

Conclusion

The different techniques of 2D NMR spectroscopy helped to assign the different arrangements of the repeating unit along the polymer chain. ^{1}H NMR spectra alone cannot give complete information due to presence of multiple peaks of broad range and therefore, along with ^{1}H NMR, ^{13}C NMR spectra

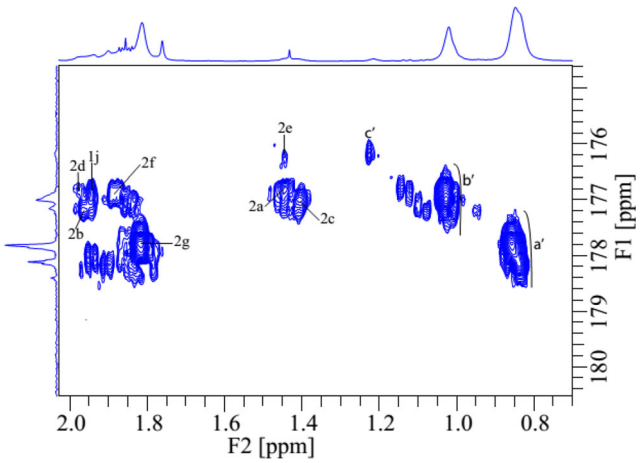

Fig. 6 2D HMBC spectrum presenting couplings of: (i) methylene protons with carbonyl carbon and (ii) α-methyl protons with carbonyl carbon

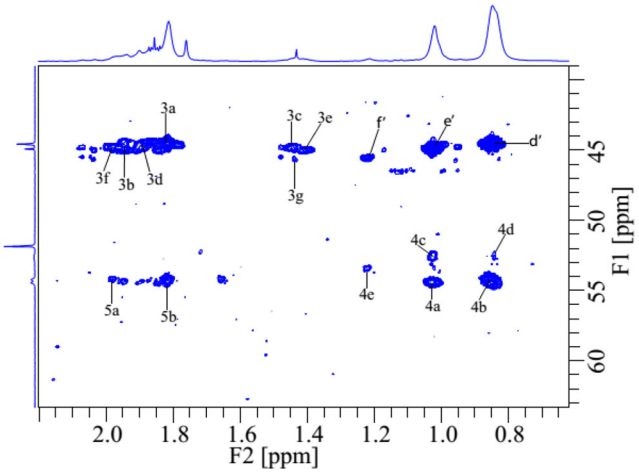

Fig. 7 2D HMBC spectrum presenting couplings of: (i) quaternary carbon with methylene protons and (ii) α-methyl protons and methylene carbon with α -methyl protons and adjacent methylene carbon

were also carried out to study the complete structure of the polymer, PMMA. 2D NMR spectra (TOCSY and HSQC) were recorded to assign the different proton attached to methylene carbon. HMBC spectra helped to assign the couplings between ^{13}C of α-methyl and ^{1}H protons of methylene group. The spectra recorded was seen to be similar to the one recorded for PMMA prepared via conventional FRP, except the crosspeaks for coupling between *mr* triad of α-methyl protons with *mrm* tetrad methylene, coupling between ^{13}C of methylene group of *mrr* tetrad with protons (H_A and H_B) of *rmr* tetrad and coupling between ^{13}C of methylene group of *mrr* tetrad with *rrr* proton in the *mrrr* pentad were not found in our prepared homopolymer PMMA via ARGET-ATRP. Hence, 2D NMR spectrum was found to be helpful to study the homopolymer of PMMA prepared via ARGET-ATRP.

Acknowledgements The Financial support from Science and Engineering Research Board (DST-SERB) (Grant no ECR/2015/000075), Govt. of India is greatly appreciated.

References

1. Matyjaszewski K, Xia J (2001) Atom transfer radical polymerization. Chem Rev 101:2921–2990
2. Hajifatheali H, Ahmadi E, Marefat M (2020) Synthesis of N-benzyl-2-(dodecylthio)-N-(2-(dodecylthio) ethyl) ethanamine: new ligand for block copolymerization of styrene and methyl methacrylate using ATRP. J Polym Res 27:22–30
3. Deoghare C, Srivastava H, Behera RN, Chauhan R (2019) Microstructure analysis of copolymers of substituted itaconimide and methyl methacrylate: experimental and computational investigation. J Polym Res 26(8):204–218
4. Rabea AM, Zhu S (2015) Modeling the influence of diffusion-controlled reactions and residual termination and deactivation on the rate and control of bulk ATRP at high conversions. Polymers. 7:819–835

5. Rabea AM, Zhu S (2014) Controlled radical polymerization at high conversion: bulk ICAR ATRP of methyl methacrylate. Ind Eng Chem Res 53:3472–3477
6. Matyjaszewski K, Tsarevsky NV, Braunecker WA, Dong H, Huang J, Jakubowski W, Kwak Y, Nicolay R, Tang W, Yoon JA (2007) Role of Cu0 in controlled/"living" radical polymerization. Macromolecules. 40:7795–7806
7. Grishin ID, Stakhi SA, Kurochkina DY, Grishin DF (2018) Controlled copolymerization of acrylonitrile with methyl acrylate and dimethyl itaconate via ARGET ATRP mechanism. J Polym Res 25:261–268
8. Ahmadian-Alam L, Haddadi-Asl V, Roghani-Mamaqani H, Hatami L, Salami-Kalajahi M (2012) Use of clay-anchored reactive modifier for the synthesis of poly (styrene-co-butyl crylate)/clay nanocomposite via in situ AGET ATRP. J Polym Res 19:9773–9784
9. Izunobi JU, Higginbotham CL (2011) Polymer molecular weight analysis by ^{1}H NMR spectroscopy. J Chem Educ 88:1098–1104
10. Brar AS, Singh G, Shankar R (2004) Structural investigations of poly(methyl methacrylate) by two-dimensional NMR. J Mol Struct 703:69–81
11. Miri MJ, Pritchard BP, Cheng HN (2011) A Versatile approach for modelling and simulating the tacticity of polymers. J Mol Model 17:1767–1780
12. Ghosh P, Das T, Nandi D (2011) Synthesis characterization and viscosity studies of Homopolymer of methyl methacrylate and copolymer of methyl methacrylate and styrene. J Solut Chem 40:67–78
13. Quinting G, Cai R (1994) High-Resoltion NMR analysis of the Tacticity of poly(n-butyl methacrylate). Macromolecules 27: 6301–6306
14. Bujak P, Henzel N, Matlengiewicz M (2007) Microstudy study of poly(tert-butyl acrylate) by ^{13}C NMR spectroscopy. J Polym Anal Charact 12:431–443
15. Hornby BD, West AG, Tom JC, Waterson C, Harrisson S, Perrier S (2010) Copper(0)-mediated living radical polymerization of methyl methacrylate in a non-polar solvent. Macromol Rapid Commun 31: 1276–1280
16. Mcbriety VJ, Douglass DC, Kwei TK (1978) Compatibility in blends of poly(methyl methacrylate) and poly(styrene-co-acrylonitrile). 2. An NMR study. Macromolecules. 11:1265–1267
17. Nguyen G, Nicole D, Swistek M, Matlengiewicz M, Wiegert B (1997) Sequence distribution of the methyl methacrylate-ethyl acrylate copolymer by ^{13}C NMR spectroscopy. Polymer 38:3455–3461
18. Pasich M, Henzel N, Matlengiewicz M (2013) Sequence distribution of poly(methyl acrylate)by incremental calculation. Int J Polym Anal Charact 18:105–118
19. Brar AS, Goyal AK, Hooda S (2009) Two dimensional NMR studies of acrylate copolymers. Pure Appl Chem 81:389–415
20. McCord EF, Anton WL, Wilczek L, Ittel SD, Nelson LTJ, Raffell KD, Hanson JE, Berge C (1994) ^{1}H and ^{13}C NMR of PMMA macromonomers and oligomers- end group and tacticity. Macromol Symp 86:47–64
21. Dhar A, Koiry P, Haloi DJ (2018) Synthesis of poly(methyl methacrylate) via ARGET ATRP and study of the effect of solvents and temperatures on its polymerization kinetics. Int J Chem Kinet 50:1–7
22. Brar AS, Kaur S (2005) Microstructure determination of methyl methacrylate and n-butyl acrylate copolymers synthesized by atom transfer radical polymerization with two-dimensional NMR spectroscopy. J Polym Sci A Polym Chem 43:1100–1118
23. Kotyk JJ, Berger PA, Remsen EE (1990) Microstructure characterization of poly(methyl methacrylate)using proton-detected heteronuclear shift-correlated NMR spectroscopy. Macromolecules 23:5167–5169
24. Kawamura T, Toshima N, Matsuzaki K (1993) Assignments of finely resolved ^{13}C NMR spectra of poly(methyl methacrylate). Makromol Chem Rapid Commun 14:719–724